Construction and Building Materials 151 (2017) 246–257

Contents lists available at ScienceDirect

Construction and Building Materials

journal homepage: www.elsevier.com/locate/conbuildmat

Shear resistance of ultra-high-performance fiber-reinforced concrete

Tri Thuong Ngo [a], Jun Kil Park [a], Sukhoon Pyo [b], Dong Joo Kim [a,*]

[a] Department of Civil and Environmental Engineering, Sejong University, 98 Gunja-Dong, Gwangjin-Gu, Seoul 05006, South Korea
[b] Korea Railroad Research Institute, 176 Railroad Museum Road, Uiwang-si, Gyeonggi-do 16105, South Korea

HIGHLIGHTS

- A newly shear testing system to investigate shear resistance of UHPFRC was proposed.
- The shear related hardening behavior, accompanied by multiple crack formation was obtained.
- The shear resistances of UHPFRCs significantly depended on both the fiber volume and *a/d*.
- The shear strengths of UHPFRCs containing 0.5 and 1.5 vol.% smooth fibers were shown to exceed the direct tensile strengths about 1.6 times.
- A theoretical model predicting the shear strength of UHPFRC based on the direct tensile strength and *a/d* was proposed.

ARTICLE INFO

Article history:
Received 26 September 2016
Received in revised form 30 May 2017
Accepted 15 June 2017

Keywords:
UHPFRC
Shear test method
Shear strength
Theoretical shear model
Shear-tension correlation
Tensile resistance

ABSTRACT

The shear resistance of ultra-high-performance fiber-reinforced concrete (UHPFRC) was investigated by using a newly proposed shear testing system. UHPFRCs displayed strain-hardening responses, in both shear and tensile testing, accompanied with multiple microcracks. The shear resistance of UHPFRCs was clearly influenced by their tensile resistance in addition to shear span to depth ratio (*a/d*). The shear strengths of UHPFRCs generally exceed the direct tensile strengths about 1.6 times. A theoretical model predicting the shear strength of UHPFRCs was proposed based on the tensile strength and *a/d* ratio.

1. Introduction

Ultra-high-performance fiber-reinforced concretes (UHPFRCs) have demonstrated superior mechanical properties, including very high compressive strengths (>150 MPa), tensile strengths (>13 MPa), tensile strain capacities (>0.3%), and energy absorption capacities (>30 kJ/m^2) even when containing only 1.5 vol% deformed steel fibers [1,2]. These properties favor the enhancement of the resistances of civil infrastructure and buildings to extreme loads, such as seismic, impact, and blast loads [3–5]. Among these extreme load conditions, impacts typically generate shear failure, rather than flexural failure, in infrastructure and buildings; shear failure is usually both brittle and catastrophic in concrete structures. However, very limited information is available regarding the shear resistance of UHPFRCs, because no standard test method exists for such concretes.

Several methods have been applied to investigate the shear resistances of UHPFRCs, as well as those of fiber-reinforced concretes (FRCs). One popular shear test method uses push-off specimens [6–11]. Two notches are made on the surface of the push-off specimen to guide shear failure between the two notch tips under tensile [6] or compressive loading [9]. Another popular method uses punch-through specimens (PTS) [12–16]. The test method to investigate shear strength of steel FRC was guided in JSCE-SF6 [12] and was modified in technique by other researchers [13–16]. In the modified PTS, two notches are made surrounding the specimen, two adjustable yokes are installed, and support plates are extended to prevent the specimen from moving. In 1967, Iosipescu proposed a shear test method using the Iosipescu specimen. This test method has been developed by several researcher to investigate shear resistance of concrete and FRC [17–19].

However, current shear test methods cannot be directly applied to investigate the shear resistance of UHPFRCs because they do not

* Corresponding author.
E-mail address: djkim75@sejong.ac.kr (D.J. Kim).

http://dx.doi.org/10.1016/j.conbuildmat.2017.06.079
0950-0618/

reflect the unique strain-hardening response, accompanied by the formation of multiple microcracks, of UHPFRCs under tension.

In this research, a new test method was proposed to investigate the shear resistance of UHPFRCs. The proposed setup was designed to provide favorable conditions for multi-shear cracking. A prism specimen without notches or reinforced steel bars was used for this setup, easing the manufacture, installation, and operation of the specimens during the test. Besides, the correlation between tensile and shear resistance, i.e., the linkage between the material levels to the structural level resistance of UHPFRCs was investigated.

This study aims to develop a fundamental understanding of the shear resistances of UHPFRCs. The specific objectives are (1) to develop a new and valid test method for the shear resistance of strain-hardening UHPFRCs with multiple microcracks, (2) to investigate the shear resistances of UHPFRCs, and (3) to discover correlations between the shear and tensile resistances of UHPFRCs.

2. Proposed shear test method for UHPFRCs

The proposed shear test system was designed to satisfy the following conditions: (1) the specimen should experience shear rather than flexural failure; (2) the results from the proposed system should reflect the unique strain-hardening characteristics, accompanied by the formation of multiple microcracks, of UHPFRCs; and, (3) the proposed system should be simple to operate.

Fig. 1 illustrates the expected shear deformation as well as the shear force diagram (SFD) and bending moment diagram (BMD) of UHPFRC specimens in the proposed test system. Both ends of the specimen are fixed while the load (P) is applied through two separate points at a distance of 60 mm, as shown in Fig. 1a. The geometry of the specimen and the load/boundary conditions are designed to generate shear failure in the UHPFRCs, rather than flexural failure, as shown in Fig. 1b. Consequently, the shear span (a), which is the distance between the loading and supporting points, is varied to generate the shear-related hardening response accompanied by the formation of multiple microcracks. As the load is applied to the specimen, the region ABCD experiences shear deformation, as shown in Fig. 1a. The engineering shear strain is defined as the change in angle between the lines $\overline{AB}$ and $\overline{AD}$, that is the vertical displacement of the middle part of the specimen (δ) per shear span (a), as shown in Eq. (1):

$$\gamma_{xy} = \alpha_x - \alpha_y = \frac{\partial u}{\partial x} + \frac{\partial v}{\partial y} = \frac{\delta}{a} \tag{1}$$

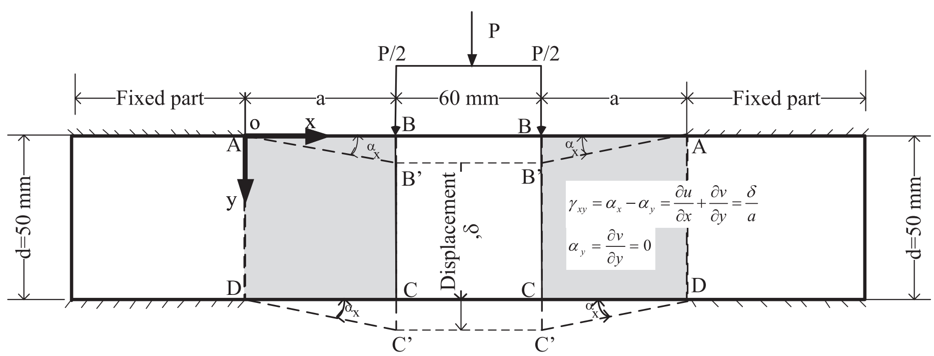

a) Set up of proposed shear test method

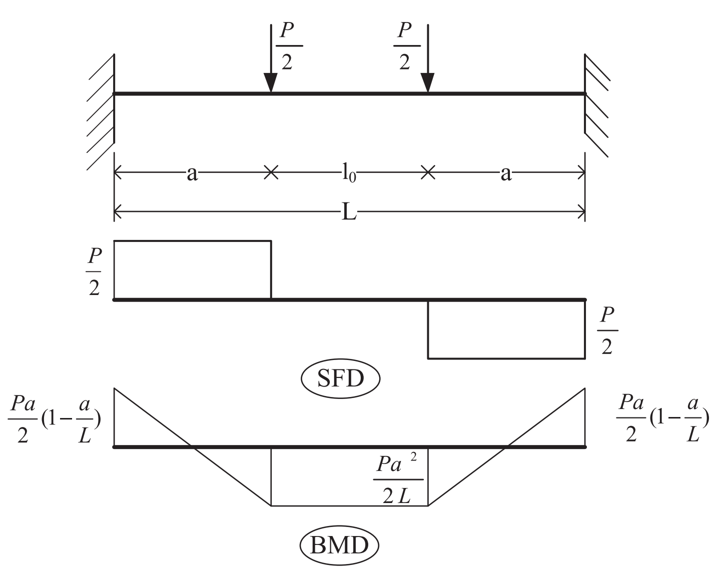

(b) Shear force and bending moment diagram

Fig. 1. Proposed shear test setup.

where γ_{xy} is the engineering shear strain, α_x is the angle between AB and A′B′, and α_y is the angle between AD and the y-axis.

3. Experiments

An experimental program was designed to investigate the shear resistances and the correlation between shear and tensile behavior of UHPFRCs. Sixteen sets of shear specimens and two sets of tensile specimens were prepared, combining different fiber volume contents and shear-span-to-depth ratios *a/d*, as illustrated in Fig. 2. The cross-sectional area of the shear and tensile specimens was constant at 50 × 50 mm. Three specimens were at least prepared per set. In the notation of the test sets, as shown in Fig. 2, the first letter designates the type of specimen ("T" for tensile and "S" for shear); the next two characters represent the fiber volume content ("05" for 0.5 vol.% fibers content). The last two characters naming the sets of shear test specimens represent the *a/d* ratio ("04" indicates *a/d* = 0.4).

3.1. Materials and specimen preparation

The composition of matrix mixture and compressive strength of the ultra-high-performance concrete (UHPC) matrix was shown in Table 1 while the properties of steel fiber was listed in Table 2 [20]. The average diameter of the silica sand is below 0.5 mm, while the average diameters of the silica fume and silica powder are about 0.1 μm and 10 μm, respectively. The silica powder and silica fume contain more than 98% SiO_2.

A Hobart type laboratory mixer with a controllable rotation speed and a 20-L capacity was used to prepare the UHPC mixture following the mixing procedure recommended in [20,21]. The cement, silica fume, silica powder, and silica sand were dry-mixed for 10 min. Water was then added to the dry mixture at intervals of 2–3 min. A superplasticizer was added gradually until the mixture showed workability and viscosity adequate for uniform fiber distribution. The fibers were dispersed by hand into the UHPC mixture and further mixed. The workability was characterized by a flow test [22] with the spread value was referenced by [23]. The mixture with fibers was carefully placed in molds using a wide scoop.

All specimens were covered by plastic sheets and stored in a laboratory at room temperature for 48 h prior to demolding. After demolding, specimens were cured in a hot water tank at the temperature of 90 ± 3 °C for 3 days. All specimens were tested at the age of 21 days in dry condition. Two layers of polyurethane were sprayed on the surfaces of the dry specimens to detect cracks more easily after failure.

3.2. Test setup and procedure

Shear tests were performed using the proposed setup and a universal test machine (UTM), as shown in Fig. 3a. During the tests, the loading speed was 1 mm/min under displacement control. The applied load was measured by a load cell in the UTM, while the vertical displacement (δ) of the specimen was measured by two LDVTs attached to the bottom of the specimen by the aluminum frame. The speed of data acquisition was 1 Hz during the shear tests.

Fig. 3b shows the tensile tests using the UTM as in the shear tests. The detail of tensile test setup refers to Tran et al. [20]. Both ends of the tensile specimen are bell-shaped and reinforced with steel wire meshes to prevent failure outside of the gauge lengths, measuring 100 mm in this study, of the specimens. The speed of loading was 1 mm/min and the data acquisition frequency was 1 Hz, as in the shear tests. Two LVDTs were attached to the specimen by an aluminum cage to measure the elongation of the specimen during testing. The load signal was measured by a load cell at the top of the specimen.

3.3. Test results

The shear load (stress) versus vertical displacement (strain) responses of the UHPFRCs are provided in Fig. 4 according to different *a/d* ratios, while the average numerical value of shear parameters are summarized in Table 3. The curves in Fig. 4 are averaged from the results of at least three specimens per set and the scale of the vertical axis in Fig. 4a differs from the others in Fig. 4. The engineering shear strain was calculated using Eq. (1), while the shear stress was calculated using Eq. (2):

$$\tau = \frac{P}{2bd} \tag{2}$$

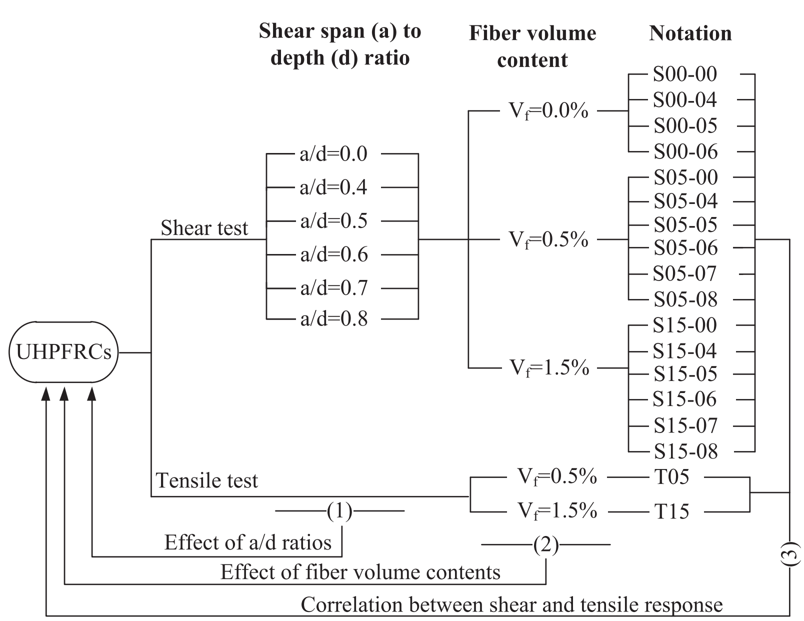

Fig. 2. Experimental program.

Table 1
Composition of matrix mixture by weight ratio and compressive strength [20].

Cement (Type I)	Silica fume	Silica sand	Silica powder	Super-plasticizer	Water	Compressive strength, (MPa)
1	0.25	1.10	0.30	0.067	0.2	180–200

Table 2
Properties of steel fiber.

Fiber type	Diameter, d_f (mm)	Length, l_f (mm)	Density, (g/cc)	Tensile strength, (MPa)	Elastic modulus, (GPa)
Smooth	0.2	19	7.90	2580	200

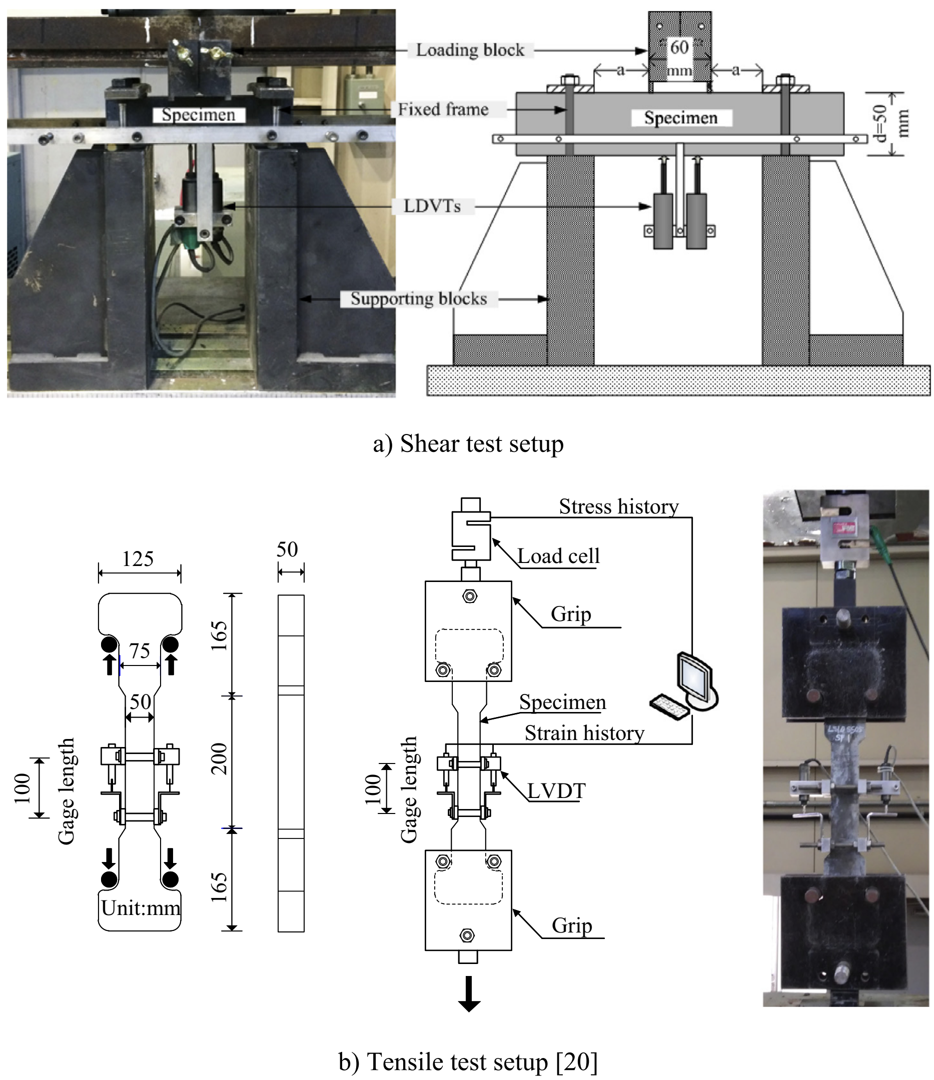

Fig. 3. Shear and tensile test setup for UHPFRCs at static rate.

where τ is the average shear stress over the cross section (MPa), P is the applied load (kN), b is the width of the specimen (mm), and d is the depth of the specimen (mm). It is noted that the engineering strain could not be calculated for $a/d = 0.0$ because the span length was zero.

The overall shape of the shear stress-versus-strain curves of the UHPFRCs depends primarily on the fiber volume contents, as shown in Fig. 4. Specimens with no fiber show sudden drops in resistance immediately after the first crack occurs, whereas the UHPFRC with fibers experience ductile failure in all tests. The UHPFRC specimens with higher fiber volumes clearly display higher shear resistances, regardless of the a/d ratios. The average ultimate shear strengths of the UHPFRCs are 7.3, 13.4, and 21.7 MPa for the addition of 0.0, 0.5, and 1.5 vol.% fiber and $a/d = 0.4$, respectively.

The failure modes of the UHPFRCs were significantly affected by the a/d ratios. The UHPFRC specimens generally experienced shear failure when the a/d ratio was between 0.4 and 0.7, but flexural

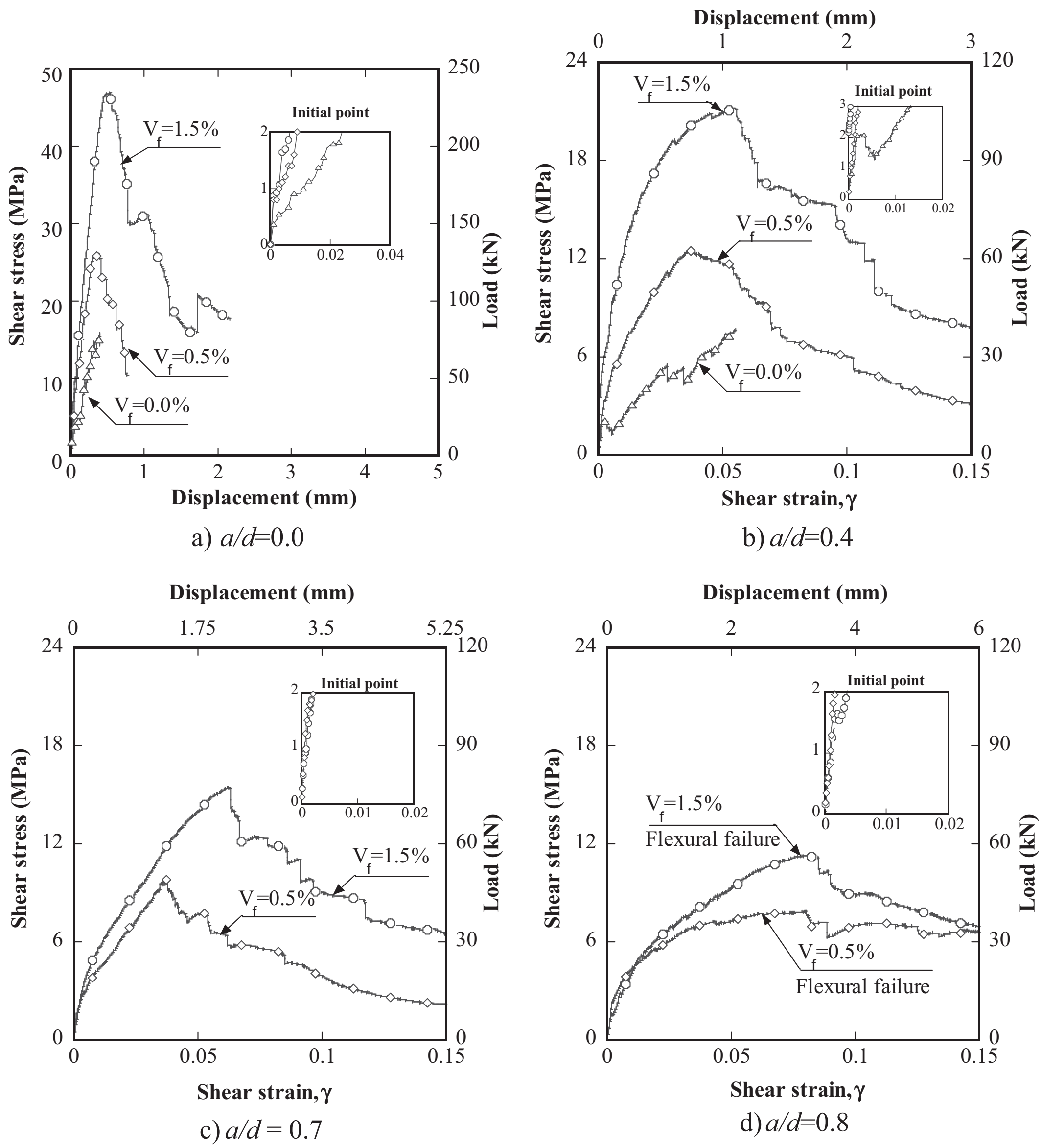

Fig. 4. Average shear stress-versus-strain curves of UHPFRCs according to different shear-span-to-depth (*a*/*d*) ratios.

failure for the *a*/*d* ratio of 0.8. The flexural failure occurs owing to the bending moment at the ends and the middle of specimen increase as the shear span (*a*) increase, as illustrated in Fig. 1b. The effects of the *a*/*d* ratios on the shear resistances of the UHPFRCs are discussed in Section 4.2.

The typical cracking behaviors of the UHPFRCs during shear testing are shown in Fig. 5. As seen in this figure, the specimens generally fail by the formation of two major inclined cracks as the *a*/*d* ratio is increased from 0.0 to 0.7, as shown in Fig. 5a and b, or three major flexural cracks for the *a*/*d* ratio of 0.8, as shown in Fig. 5c. The inclined shear cracks connect the inner edge of the supporting block and the outer edge of the loading block. The specimen of the S05-04 series produces only two major inclined cracks, whereas the specimen of the S15-07 series produces multiple microcracks in addition to the two major inclined cracks.

Fig. 6 provides the tensile stress-versus-strain responses of the UHPFRCs, while the tensile parameters of the UHPFRCs are summarized in Table 3. The UHPFRCs with 1.5 vol.% steel fibers (T15) demonstrate tension-related strain-hardening behavior, whereas those with 0.5 vol.% steel fibers (T05) show tension-related strain-softening responses. The average tensile strength of T15 is 11.9 MPa, while that of T05 is 7.5 MPa. Moreover, the strain capacity (6.95×10^{-3}) of T15 is much higher than that (0.5×10^{-3}) of T05. The typical cracking behavior of UHPFRCs in tension is shown in Fig. 7. Fig. 7a shows the cracking behavior of the strain-softening T05 and Fig. 7b shows the formation of multiple microcracks in strain-hardening T15.

4. Discussions

4.1. Shear stress-versus-strain responses of UHPFRCs obtained using the proposed test method

The typical shear stress-versus-strain responses of UHPFRCs as obtained by the proposed test system are illustrated in Fig. 8. Both UHPFRCs containing 0.5 and 1.5 vol.% steel fibers display similarly shaped responses. The initial portion of the curves is linear prior to the first shear cracking; afterwards, both UHPFRCs show nonlinear

Table 3
Shear test results.

Test series	Fiber volume content (%)	Shear span to depth ratio (a/d)	Specimen	Ultimate shear strength, τ_{max} (MPa)	Shear strain capacity, γ_{max}	Note
S00-00	0.0	0.0	1	16.46	–	Failed in shear mode
			2	17.55	–	
			3	17.47	–	
			4	16.12	–	
			5	16.41	–	
			6	17.38	–	
			Aver.	***16.90***	–	
			Standard deviation	***0.64***	–	
S05-00	0.5		1	27.20	–	Failed in shear mode
			2	26.73	–	
			3	27.01	–	
			4	25.64	–	
			5	26.78	–	
			Aver.	***26.67***	–	
			Standard deviation	***0.61***	–	
S15-00	1.5		1	47.56	–	Failed in shear mode
			2	46.95	–	
			3	47.95	–	
			4	46.83	–	
			Aver.	***47.32***	–	
			Standard deviation	***0.53***	–	
S00-04	0.0	0.4	1	7.68	0.055	Failed in shear and flexure mode
			2	7.47	0.028	
			3	6.86	0.046	
			Aver.	***7.34***	***0.043***	
			Standard deviation	***0.42***	***0.014***	
S05-04	0.5		1	12.61	0.040	Failed in shear mode
			2	13.87	0.034	
			3	13.65	0.054	
			4	13.97	0.038	
			5	12.32	0.054	
			6	14.10	0.044	
			Aver.	***13.42***	***0.044***	
			Standard deviation	***0.76***	***0.008***	
S15-04	1.5		1	21.44	0.052	Failed in shear mode
			2	21.31	0.055	
			3	21.85	0.053	
			4	22.30	0.061	
			5	21.79	0.045	
			Aver.	***21.74***	***0.053***	
			Standard deviation	***0.38***	***0.006***	
S00-05	0.0	0.5	1	5.93	0.039	Failed in shear and flexure mode
			2	5.91	0.030	
			3	5.79	0.021	
			4	7.50	0.033	
			5	6.71	0.037	
			Aver.	***6.37***	***0.032***	
			Standard deviation	***0.73***	***0.007***	
S05-05	0.5		1	11.82	0.066	Failed in shear mode
			2	11.80	0.067	
			3	12.10	0.048	
			4	12.51	0.042	
			5	12.26	0.038	
			Aver.	***12.10***	***0.052***	
			Standard deviation	***0.30***	***0.014***	
S15-05	1.5		1	21.15	0.063	Failed in shear mode
			2	19.82	0.052	
			3	20.99	0.053	
			4	20.80	0.060	
			5	20.35	0.061	
			Aver.	***20.62***	***0.058***	
			Standard deviation	***0.54***	***0.005***	
S00-06	0.0	0.6	1	5.52	0.016	Failed in shear and flexure

(*continued on next page*)

Table 3 (*continued*)

Test series	Fiber volume content (%)	Shear span to depth ratio (a/d)	Specimen	Ultimate shear strength, τ_{max} (MPa)	Shear strain capacity, γ_{max}	Note
			2	5.53	0.018	mode
			3	5.86	0.020	
			Aver.	***5.64***	***0.018***	
			Standard deviation	***0.19***	***0.002***	
S05-06	0.5		1	11.21	0.075	Failed in shear mode
			2	11.51	0.047	
			3	10.83	0.067	
			4	10.66	0.056	
			Aver.	***11.05***	***0.061***	
			Standard deviation	***0.38***	***0.012***	
S15-06	1.5		1	18.37	0.091	Failed in shear mode
			2	18.46	0.075	
			3	19.02	0.081	
			Aver.	***18.61***	***0.082***	
			Standard deviation	***0.35***	***0.008***	
S05-07	0.5	0.7	1	10.95	0.052	Failed in shear mode
			2	10.90	0.040	
			3	10.87	0.037	
			4	10.14	0.039	
			Aver.	***10.71***	***0.042***	
			Standard deviation	***0.39***	***0.007***	
S15-07	1.5		1	16.28	0.061	Failed in shear mode
			2	14.70	0.063	
			3	14.99	0.063	
			4	16.47	0.066	
			Aver.	***15.61***	***0.063***	
			Standard deviation	***0.89***	***0.002***	
S05-08	0.5	0.8	1	8.79	0.071	Failed in flexure mode
			2	6.88	0.089	
			3	8.18	0.068	
			Aver.	***7.95***	***0.076***	
			Standard deviation	***0.98***	***0.011***	
S15-08	1.5		1	11.39	0.089	Failed in flexure mode
			2	11.67	0.076	
			3	11.24	0.089	
			Aver.	***11.43***	***0.084***	
			Standard deviation	***0.22***	***0.007***	

responses up to the peaks of the curves. Both UHPFRCs demonstrate ductile failure, even in the specimen with only 0.5 vol.% fibers, rather than tensile failure. As illustrated in Fig. 8, the peak shear stress in the curve is labeled as the ultimate shear strength (τ_{max}), while the shear strain at the peak value is labeled as the shear strain capacity (γ_{max}). The values for both τ_{max} and γ_{max} of the UHPFRCs are summarized in Table 3.

The UHPFRCs with only 0.5% fibers interestingly show shear-related hardening responses, as shown in Figs. 4 and 8, although they demonstrate strain-softening in tension, as shown in Fig. 6. These different responses under shear and tensile deformation can be attributed to the different fiber bridging mechanisms in these modes. The fiber bridging mechanism of UHPFRCs in tension is mostly fiber pullout, whereas that in shear follows the dowel effects of short fibers crossing the cracked sections because of the different fiber orientations during the casting of the specimens, as illustrated in Fig. 9.

The cracking behaviors of the UHPFRCs in shear were also clearly influenced by the fiber volume contents: the specimens with 1.5 vol.% fibers experienced the formation of multiple microcracks, while the specimens with 0.5 vol.% fibers exhibited localized single instances of cracking, as shown in Figs. 5 and 8, respectively. Although the UHPFRCs in shear showed different cracking behaviors with different fiber volumes, all specimens eventually failed with two inclined major cracks, as shown in Fig. 5. The failure pattern with inclined cracks is very similar to the typical shear failure observed in normal concrete [24] or the punching shear failure of UHPFRC slabs [25].

Overall, the obtained results from the proposed test method, as shown in Figs. 4, 5, and 8, indicated that the proposed method could successfully reflect the shear-related strain-hardening response, accompanied by the formation of multiple microcracks, characteristic of UHPFRCs in shear resistance. Consequently, it can be concluded that the proposed test method is valid for investigating the shear resistance behaviors of strain-hardening UHPFRCs or other FRCs.

4.2. Shear resistance of UHPFRCs

The effect of *a/d* ratio on the shear strength τ_{max} of the UHPFRC is shown in Fig. 10. The τ_{max} of the UHPFRCs with 1.5 vol.% fibers is decreased from 47.3 to 15.6 MPa as the *a/d* ratio is increased from 0.0 to 0.7, while those of UHPFRCs containing 0.5 vol.% fibers decreased from 26.7 to 10.7 MPa. Moreover, the shear strength of

a) S05- 04

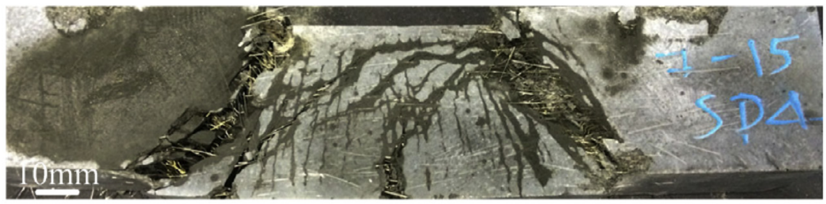

b) S15- 07

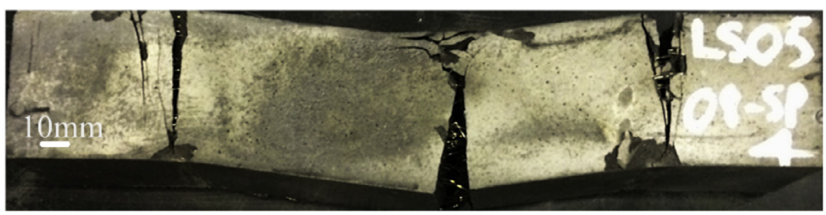

c) S05- 08

Fig. 5. Cracking behaviors of UHPFRCs during shear test.

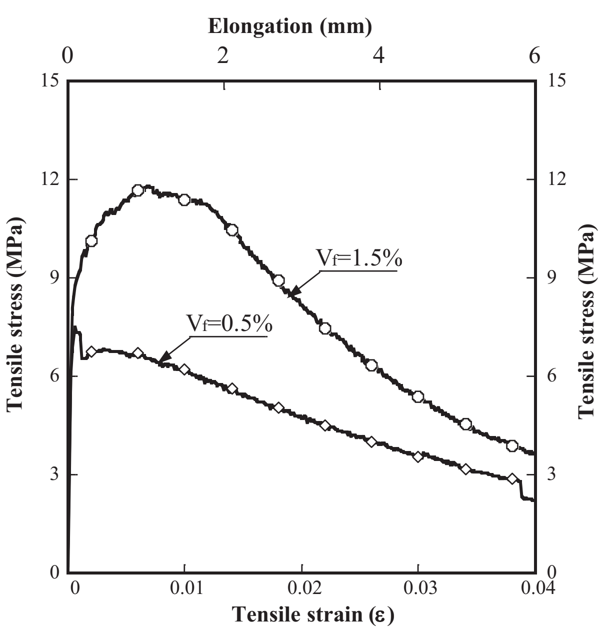

Fig. 6. Average tensile stress–strain curves.

the UHPFRC without fiber was also significantly influenced by the a/d ratio. The decrease of τ_{max} with increasing a/d ratio has been reported by several researchers [26,27].

The shear strengths of the UHPFRCs were also significantly affected by the addition of steel fibers, as shown in Figs. 4 and 8: increased fiber contents correlate to increased shear strength. Similar trends in the enhancement of shear strength by the addition of steel fibers has been reported by other researchers [8,14]. The addition of fibers is effective in enhancing both the tensile and shear resistance of UHPFRCs.

A theoretical model is proposed here to predict the shear strengths of UHPFRCs, as shown in Fig. 11, based on the measured tensile resistance and a/d ratio of a specimen. The following assumptions were considered in the proposed model: (1) Specimens predominantly experience shear failure; (2) Shear failure is governed by diagonal tensile failure along the A-B direction, as described in Fig. 11; and (3) The tensile resistance of UHPFRCs is governed by the fiber pullout resistance.

As seen in Fig. 11, half of a given specimen was modeled because it is symmetrical. The crack slip shear force (F_a), tensile forces of the fibers (F_{fb}), and reaction force at the support ($P/2$) were considered in modelling.

The F_{fb} is the total resistance of all fibers across the crack. Since the fibers are randomly distributed across the crack, F_{fb} can be calculated using Eq. (3):

$$\begin{aligned} F_{fb} &= \int_0^{L_s} N_f \times \left(\frac{1}{\pi}\int_0^{\pi} (E_f A_f \varepsilon_{fb}) \sin\alpha d\alpha\right) \\ &= \int_0^{L_s} \left(\frac{V_f b dL_s}{A_f}\right) \times \left(\frac{2}{\pi} E_f A_f \frac{l_f \tau}{d_f E_f}\right) \\ &= \frac{2ab}{\pi \cos\theta} \times \frac{l_f V_f}{d_f} \times \tau \end{aligned} \tag{3}$$

where E_f, A_f, ε_{fb}, and N_f are the elastic modulus, area, strain, and number of fibers across the crack, respectively [28]. In Eq. (3), the strain ε_{fb} can be calculated by assuming that the net fiber pull-out length is about $l_f/4$ [29]. τ represents the equivalent bond strength at the interface between the fiber and the concrete matrix.

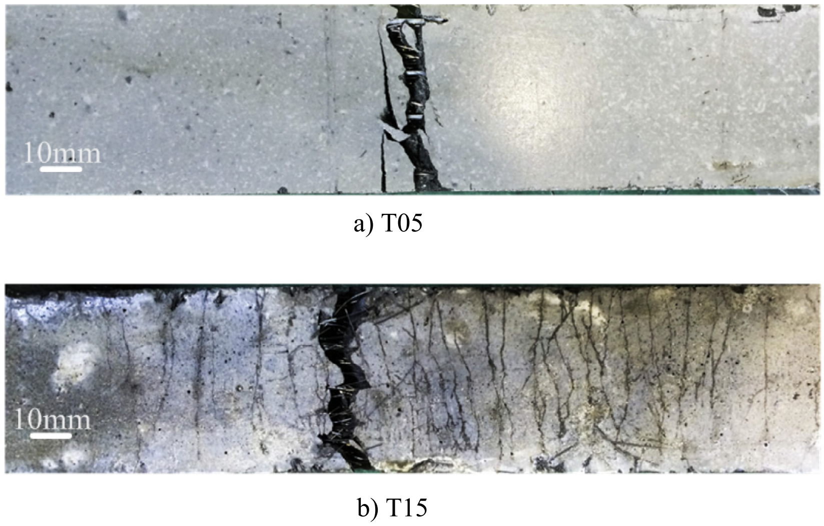

Fig. 7. Cracking behaviors of UHPFRCs in tension.

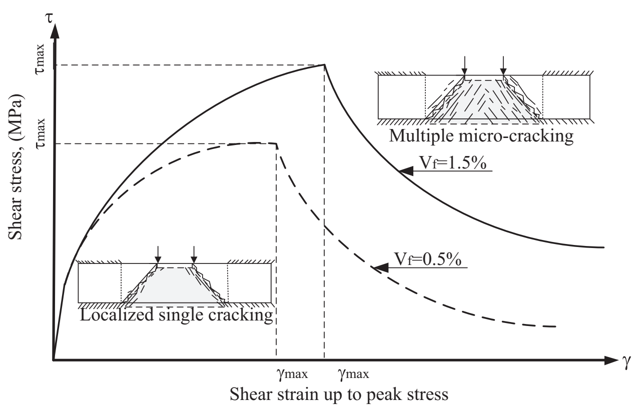

Fig. 8. Typical shear stress–strain responses of UHPFRCs.

The post-cracking tensile strengths of UHPFRCs can be theoretically predicted, according to Naaman [30], using Eq. (4):

$$\sigma_{pc} = \lambda\tau\frac{l_f}{d_f}V_f \tag{4}$$

where λ is a coefficient considering the group effect, fiber orientation, averaged embedded length, and spalling effect [31].

Substituting Eq. (4) into Eq. (3) yields:

$$F_{fb} = \frac{2ab}{\pi\cos\theta}\times\frac{\sigma_{pc}}{\lambda} \tag{5}$$

Based on force equilibrium,

$$F_{fb} = \frac{P}{2}\cos\theta \tag{6}$$

By combining Eqs. (5) and (6),

$$\frac{P}{2} = \frac{2ab}{\pi}\times\frac{\sigma_{pc}}{\lambda}\times(1+\tan^2\theta) \tag{7}$$

Consequently, the shear strength is calculated by dividing both sides of Eq. (7) by the cross-sectional area (bd) of the specimen:

$$\tau_{\max} = \frac{2}{\pi}\times\frac{\sigma_{pc}}{\lambda}\times\left(a/d+\frac{1}{a/d}\right) \tag{8}$$

Eq. (8) clearly demonstrates the dependency of the shear strength of UHPFRC on both the post-cracking tensile strength and the a/d ratio. To evaluate the proposed model, the test results were compared to the model, as summarized in Table 4. Notably, the proposed model is not applicable for the case of $a/d = 0.0$, because the failure mode of the specimen was assumed to be diagonal tensile failure.

The theoretical shear strength (τ_{th}) calculated from Eq. (8) for the UHPFRCs is compared with the experimental results (τ_{ex}) in Table 5. In calculating τ_{th}, the coefficient λ is assumed to be 0.96 [31]. The value of $\lambda = 0.96$ is used to calculate the lower bound value for UHPFRCs containing 0.5 and 1.5 vol.% smooth fibers in this study, because higher fiber contents typically produce lower values of λ [31]. In addition, the post-cracking tensile strengths used to calculate τ_{th} are from Table 4: σ_{pc} was 11.9 and 7.6 MPa for the UHPFRCs with 1.5 and 0.5 vol.% fibers, respectively. As demonstrated in Table 5, the calculated τ_{th} are in good agreement with τ_{ex}. As the a/d ratio is increased from 0.4 to 0.7, the ratio between τ_{ex} and τ_{th} varies between 0.92 and 1.00 for UHPFRCs with 0.5 vol.% fibers and between 0.93 and 1.04 for the UHPFRCs with 1.5 vol.%, respectively. The standard deviation (SD) and coefficient of variation (COV) are also shown in Table 5.

4.3. Correlation between tensile and shear strength of UHPFRCs

The shear strengths of the UHPFRCs, normalized by the post-cracking tensile strengths, are shown in Fig. 12 according to different a/d ratio. As seen in Fig. 12, the shear strengths (τ_{max}) of the UHPFRCs are always higher than the tensile strengths (σ_{pc}), regardless of the a/d ratio for the specimens. However, as the a/d ratio is increased from 0.4 to 0.7, the τ_{max}/σ_{pc} of the UHPFRCs with 0.5 vol.% fibers is decreased from 1.8 to 1.4, while that of the UHPFRCs with 1.5 vol.% fibers is decreased from 1.8 to 1.3. The average value of the normalized shear strengths (τ_{max}/σ_{pc}) for both UHPFRCs containing 0.5 and 1.5 vol.% steel fibers is about 1.6. This value is in excellent agreement with previous results reported by van Zijl [17] and Li et al. [18] for fiber reinforced cementitious composites.

The test results are also compared with the theoretical normalized shear strength (τ_{max}/σ_{pc}) using Eq. (8), as is shown in Fig. 12. The theoretical τ_{max}/σ_{pc} ratios of the UHPFRCs containing 0.5 and 1.5 vol.% fiber are identical for specific a/d ratios because equal values of λ are assumed in the calculation. Similar to the experimental results, the theoretical τ_{max}/σ_{pc} ratio is also decreased as the a/d ratio is increased from 0.4 to 0.7. Consequently, the proposed theoretical model is considered valid for estimating the shear strengths of UHPFRCs.

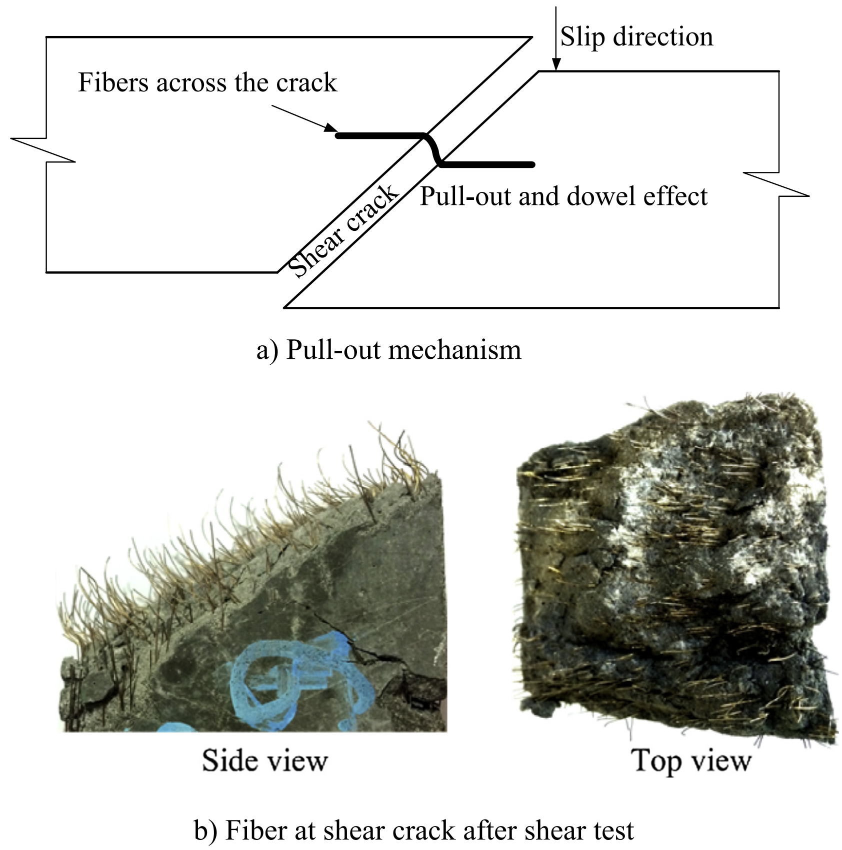

Fig. 9. Pull-out mechanism of fiber across cracks during shear test.

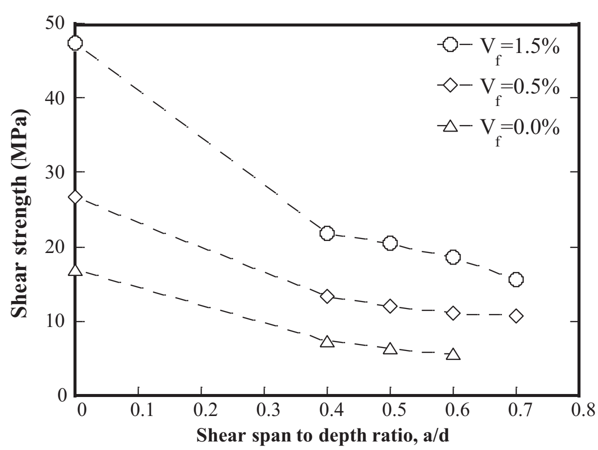

Fig. 10. Effect of *a*/*d* ratio on shear strength of UHPFRCs.

5. Conclusions

In this study, a comprehensive experimental program was undertaken to validate a proposed test method for investigating the shear resistances of UHPFRCs. In addition, the shear resistances, as well as the correlations between the shear and tensile resistances, of UHPFRCs were investigated. The following observations and conclusions could be drawn from the study:

1. The proposed test method is valid for investigating the shear resistances of strain-hardening UHPFRCs or other FRCs. The strain-hardening behavior, accompanied by multiple crack formation, characteristic of UHPFRCs in tension can be measured, even in shear failure, by the proposed test system.
2. The shear resistances of UHPFRCs significantly depended on both the fiber volume and shear-span-to-depth ratio (*a*/*d*). Higher *a*/*d* ratios promoted lower shear strengths, while higher fiber volumes promoted higher shear strengths. The shear

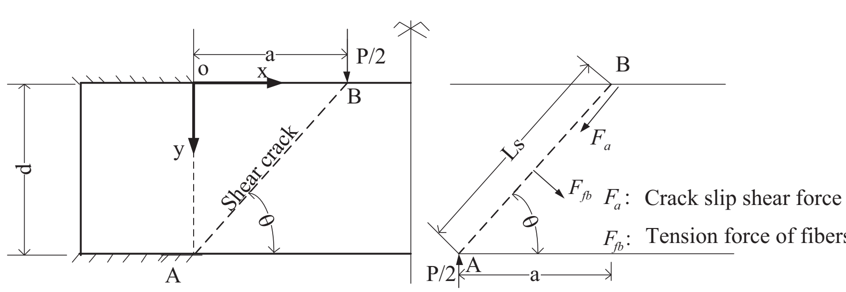

Fig. 11. Theoretical model predict shear strength of UHPFRCs.

Table 4
Tensile test results.

Test series	Specimen	First cracking strength, α_{cc} (MPa)	Post cracking strength, σ_{pc} (MPa)	Strain capacity, ε_{pc}
T15	1	8.76	11.88	0.006
	2	8.22	11.71	0.007
	3	9.15	12.22	0.012
	4	9.18	11.92	0.003
	Average	***8.83***	***11.93***	***0.007***
	Standard deviation	***0.45***	***0.21***	***0.004***
T05	1	7.70		0.0006
	2	7.62		0.0005
	3	7.12		0.0004
	Average	***7.48***		***0.0005***
	Standard deviation	***0.31***		***0.0001***

Table 5
Ultimate shear strength of UHPFRCs.

a/d	$V_f = 0.5\%$			$V_f = 1.5\%$		
	τ_{ex} (MPa)	τ_{th} (MPa)	τ_{ex}/τ_{th}	τ_{ex} (MPa)	τ_{th} (MPa)	τ_{ex}/τ_{th}
0.4	13.42	14.58	0.92	21.74	22.95	0.95
0.5	12.10	12.57	0.96	20.62	19.79	1.04
0.6	11.05	11.40	0.97	18.61	17.94	1.04
0.7	10.71	10.70	1.00	15.61	16.85	0.93
	SD		***0.03***	SD		***0.06***
	COV		***3.45%***	COV		***6.09%***

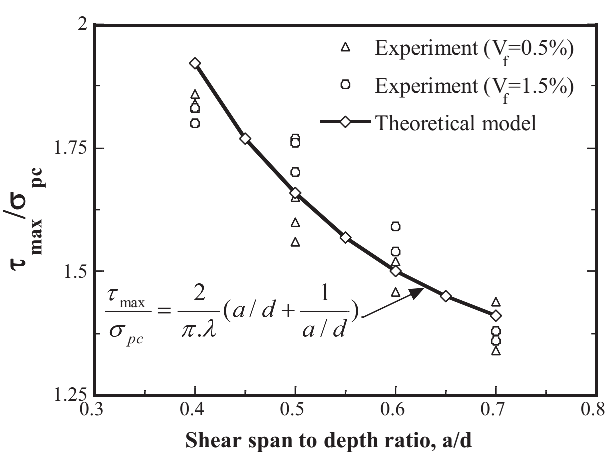

Fig. 12. Normalized shear strength of UHPFRCs.

strengths of UHPFRCs with 1.5 vol.% fibers decreased from 47.3 to 15.6 MPa as the *a/d* ratio increased from 0.0 to 0.7, while those of UHPFRCs containing 0.5 vol.% fibers decreased from 26.7 to 10.7 MPa.

3. UHPFRC with 1.5 vol% steel fibers demonstrated strain-related hardening in both shear and tensile failure, whereas the UHPFRC with 0.5 vol.% steel fibers showed strain-hardening in shear failure but strain-softening in tensile failure. The shear strengths of UHPFRCs containing 0.5 and 1.5 vol.% smooth fibers were shown to exceed the direct tensile strengths about 1.6 times.
4. The good agreement between the calculated and measured results showed that the proposed theoretical model, based on the direct tensile resistance and shear-span-to-depth ratio, could be valid for estimating the shear resistances of UHPFRCs.

Acknowledgements

This research was supported by a grant from a Construction Technology Research Project (17SCIP-B128706-01) funded by the Ministry of Land, Infrastructure and Transport. The opinions expressed in this paper are those of authors and do not necessarily reflect the views of the sponsors.

References

[1] K. Wille, D.J. Kim, A.E. Naaman, Strain-hardening UHP-FRC with low fiber contents, Mater. Struct. 44 (2011) 583–598, http://dx.doi.org/10.1617/s11527-010-9650-4.
[2] M. Xu, K. Wille, Fracture energy of UHP-FRC under direct tensile loading applied at low strain rates, Compos. Part B 80 (2015) 116–125, http://dx.doi.org/10.1016/j.compositesb.2015.05.031.
[3] S.H. Park, D.J. Kim, S.W. Kim, Investigating the impact resistance of ultra-high-performance fiber-reinforced concrete using an improved strain energy impact test machine, Constr. Build. Mater. 125 (2016) 145–159, http://dx.doi.org/10.1016/j.conbuildmat.2016.08.027.
[4] S. Pyo, S. El-Tawil, Capturing the strain hardening and softening responses of cementitious composites subjected to impact loading, Constr. Build. Mater. 81 (2015) 276–283, http://dx.doi.org/10.1016/j.conbuildmat.2015.02.028.
[5] Z. Rong, W. Sun, Experimental and numerical investigation on the dynamic tensile behavior of ultra-high performance cement based composites, Constr. Build. Mater. 31 (2012) 168–173, http://dx.doi.org/10.1016/j.conbuildmat.2011.12.058.
[6] A.H. Mattock, N.M. Hawkins, Shear transfer in reinforced concrete—recent research, J. Prestressed Concr. Inst. 17 (1972) 55–75.
[7] M. Valle, O. Büyüköztürk, Behavior of fiber reinforce high-strength concrete under direct shear, ACI Mater. J. 90 (1993) 122–133.
[8] A.R. Khaloo, N. Kim, Influence of concrete and fiber characteristics on behavior of steel fiber reinforced concrete under direct shear, ACI Mater. J. 94 (1997).
[9] B. Barragán, R. Gettu, L. Agulló, R. Zerbino, Shear failure of steel fiber-reinforced concrete based on push-off tests, ACI Mater. J. 103 (2006) 251–257.
[10] S.G. Millard, T.C.K. Molyneaux, S.J. Barnett, X. Gao, Dynamic enhancement of blast-resistant ultra high performance fibre-reinforced concrete under flexural and shear loading, Int. J. Impact Eng. 37 (2010) 405–413, http://dx.doi.org/10.1016/j.ijimpeng.2009.09.004.
[11] J. Navarro-Gregori, E.J. Mezquida-Alcaraz, P. Serna-Ros, J. Echegaray-Oviedo, Experimental study on the steel-fibre contribution to concrete shear behaviour, Constr. Build. Mater. 112 (2016) 100–111, http://dx.doi.org/10.1016/j.conbuildmat.2016.02.157.
[12] JSCE-SF6, Method of Test for Shear strength of Steel Fiber Reinforced Concrete, (1990) 67–9.
[13] G. Appa Rao, a. Sreenivasa Rao, Toughness indices of steel fiber reinforced concrete under mode II loading, Mater. Struct. 42 (2009) 1173–1184, http://dx.doi.org/10.1617/s11527-009-9543-6.
[14] F. Soltanzadeh, J.A.O. Barros, R.F.C. Santos, High performance fiber reinforced concrete for the shear reinforcement: experimental and numerical research, Constr. Build. Mater. 77 (2015) 94–109, http://dx.doi.org/10.1016/j.conbuildmat.2014.12.003.

[15] B. Boulekbache, M. Hamrat, M. Chemrouk, S. Amziane, Influence of yield stress and compressive strength on direct shear behaviour of steel fibre-reinforced concrete, Constr. Build. Mater. 27 (2012) 6–14, http://dx.doi.org/10.1016/j.conbuildmat.2011.07.015.

[16] N. Banthia, F. Majdzadeh, J. Wu, V. Bindiganavile, Fiber synergy in Hybrid Fiber Reinforced Concrete (HyFRC) in flexure and direct shear, Cem. Concr. Compos. 48 (2014) 91–97, http://dx.doi.org/10.1016/j.cemconcomp.2013.10.018.

[17] G.P.A.G. van Zijl, Improved mechanical performance: shear behaviour of strain-hardening cement-based composites (SHCC), Cem. Concr. Res. 37 (2007) 1241–1247, http://dx.doi.org/10.1016/j.cemconres.2007.04.009.

[18] V.C. Li, D.K. Mishra, A.E. Naaman, J.K. Wight, J.M. Lafave, H. Wu, Y. Inada, On the shear behavior of engineered cementitious composites, Adv. Cem. Based Mater. 1 (1993) 142–149.

[19] M. Derradj, Æ.S. Kaci, Numerical study of compact shear (Mode II) type test specimen geometry, (2008) 1203–1210, doi:10.1617/s11527-007-9318-x.

[20] N.T. Tran, T.K. Tran, D.J. Kim, High rate response of ultra-high-performance fiber-reinforced concretes under direct tension, Cem. Concr. Res. 69 (2015) 72–87, http://dx.doi.org/10.1016/j.cemconres.2014.12.008.

[21] J.J. Park, S.T. Kang, K.T. Koh, S.W. Kim, Influence of the ingredients on the compressive strength of UHPC as a fundamental study to optimize the mixing proportion, Proceeding Second Int. Symp. Ultra High Perform, Concr. Kassel, Ger. (2008) 105–102.

[22] ASTM International, ASTM C 1437 Standard Test Method for Flow of Hydraulic Cement Mortar, (2001) 1–2.

[23] K. Wille, A.E. Naman, G.J. Parra-Montesinos, Ultra - high performance concrete with compressive strength exceeding 150 MPa (22ksi): a simpler way, ACI Mater. J. 108 (2011) 46–53.

[24] M.T.B. Ridha Boulifa, Mohamed Lai Samai, A new technique for studying the behaviour of concrete in shear, J. King Saud. Univ. Sci. 25 (2013) 149–159, http://dx.doi.org/10.1016/j.jksues.2012.07.001.

[25] A.M.T. Hassan, G.H. Mahmud, S.W. Jones, C. Whitford, A new test method for investigating punching shear strength in Ultra High Performance Fibre Reinforced Concrete (UHPFRC) slabs, Compos. Struct. 131 (2015) 832–841, http://dx.doi.org/10.1016/j.compstruct.2015.06.044.

[26] J. Hegger, G. Bertram, Shear carrying capacity of ultra-high performance concrete beams, Inst. Struct. Concr. Ta RWTH Aachen .... (2008) 341–348. http://www.abece.com.br/web/restrito/restrito/pdf/ch049.pdf.

[27] M.H.A. Omar, Q. Aziz, Shear strength and behavior of ultra-high performance fiber reinforced concrete (UHPC) deep beams without web reinforced reinforcement, Int. J. Civ. Eng. 2 (2013).

[28] T. Nyomboi, H. Matsuda, R. Hirayama, H. Nishida, Theoretical prediction of shear strength evolution in steel fibre reinforced concrete beams without stirrups, Rep. Fac. Eng. Nagasaki Univ. 38 (2008) 20–27.

[29] D.H. Lim, B.H. Oh, Experimental and theoretical investigation on the shear of steel fibre reinforced concrete beams, Eng. Struct. 21 (1999) 937–944.

[30] A.E. Naaman, Tensile strain-hardening FRC composites: historical evolution since the 1960, Adv. Constr. Mater. Part II (2007) 181–202.

[31] K. Wille, S. El-tawil, A.E. Naaman, Properties of strain hardening ultra high performance fiber reinforced concrete (UHP-FRC) under direct tensile loading, Cem. Concr. Compos. 48 (2014) 53–66, http://dx.doi.org/10.1016/j.cemconcomp.2013.12.015.